Journal of Energy and Environmental Sustainability, 2 (2016) 1-6

An official publication of the International Society for Energy, Environment and Sustainability (ISEES)

Journal of Energy and Environmental Sustainability

Journal homepage : www.jees.in

Validation of a Novel Scaling Methodology for CFD Simulations of a Spouted Fluidized Bed with γ-Al_2O_3 Particles

Subhodeep Banerjee, Ramesh K. Agarwal*

Department of Mechanical Engineering and Materials Science, Washington University in St. Louis, 1 Brookings Drive, St. Louis, MO 63130

A R T I C L E I N F O

Received : 15 August 2016
Revised : 26 September 2016
Accepted : 27 September 2016

Keywords:
Chemical looping combustion, CFD simulation, fluidized bed scaling, dynamic similarity

A B S T R A C T

Chemical-looping combustion (CLC) is a next generation combustion technology that shows great promise as a solution for the need of high-efficiency low-cost carbon capture from fossil fueled power plants. The spouted fluidized bed setup provides several advantages when solid coal is used as fuel for CLC. The Lagrangian particle tracking approach known as Discrete Element Method (DEM) coupled with a computational fluid dynamics (CFD) solution of the flow field provides an effective means of simulating the behavior of a spouted fluidized bed. Given the high computing cost of CFD-DEM, it is necessary to develop a scaling methodology based on the principles of dynamic similarity that can be applied to a CFD-DEM simulation to expand the scope of this approach to larger CLC systems up to the industrial scale. A novel scaling methodology based on the terminal velocity was proposed and shown to improve the accuracy of the simulation results compared to existing scaling methodologies in the literature in a cold-flow simulation of a spouted fluidized experiment with glass beads. In this paper, the scaling methodologies are applied to a spouted fluidized bed consisting of γ-Al_2O_3 particles to affirm the validity of the proposed scaling law for materials with different physical properties than glass beads.

Nomenclature

Ar	=	Archimedes number
C_D	=	particle drag coefficient
d_p	=	particle diameter, m
$g, \mathbf{g}$	=	gravitational acceleration, m/s²
G_s	=	solids mass flux, kg/(m²-s)
F_C	=	collision force per unit particle mass, m/s²
F_D	=	net drag coefficient per unit particle mass, 1/s
Fr	=	Froude number
K	=	particle spring constant, N/m
L	=	bed length or height, m
n	=	particle scale factor
p	=	pressure, Pa
r	=	geometry scale factor
Re_p	=	particle Reynolds number
$u, \mathbf{u}$	=	velocity, m/s
u_{bg}	=	background velocity, m/s
u_{mf}	=	minimum fluidization velocity, m/s
u_{sp}	=	spout velocity, m/s
u_0	=	superficial gas velocity, m/s
u_{12}	=	relative velocity of collision pair, m/s
$v_{r,p}$	=	terminal velocity correction factor

Greek letters

α	=	volume fraction
γ	=	collision damping coefficient, kg/s
δ	=	particle overlap during collision, m
η	=	particle coefficient of restitution
μ	=	dynamic viscosity, kg/(m-s)
ρ	=	density, kg/m³
$\bar{\bar{\tau}}_f$	=	shear stress tensor, Pa
ϕ	=	particle sphericity

Subscripts

ex	=	exact model
f	=	fluid phase
p	=	particle
sc	=	scaled model

1. Introduction

As a result of the rapid combustion of fossil fuels, the level of CO_2 in the atmosphere has risen by almost 30% compared to the pre-industrial times and the Intergovernmental Panel on Climate Change (2007) has reported that the "warming of the climate system is unequivocal" and that "most of the observed increase in global average temperatures since the mid-20th century is very likely due to the observed increase in anthropogenic greenhouse gas concentrations." As a result, addressing carbon emissions from power plants has become an active area of research.

One technology that has shown great promise for high-efficiency low-cost carbon capture is chemical-looping combustion (CLC). The CLC process utilizes dual fluidized bed reactors termed the air reactor and the fuel reactor and a metal oxide oxygen carrier that circulates between the two reactors, as illustrated in Figure 1. The primary advantage of CLC is that fuel combustion in the fuel reactor takes place in the absence of air

* *Corresponding Author: Email: rka@wustl.edu*

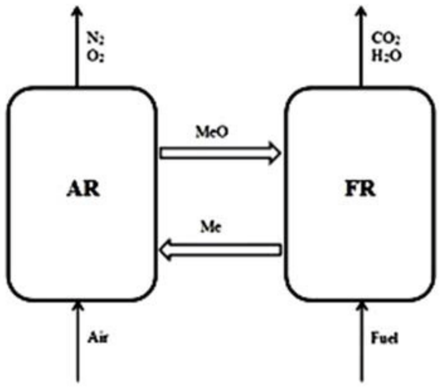

Figure 1. Schematic representation of a chemical-looping combustion system with interconnected fluidized beds (AR = air reactor, FR = fuel reactor)

using oxygen provided by the oxygen carrier; the flue stream from the fuel reactor is not contaminated or diluted by other gases such as nitrogen. This provides a high-purity carbon dioxide stream available for capture at the fuel reactor outlet without the need for an energy-expensive gas separation process. The reduced oxygen carrier from the fuel reactor is pneumatically transported to the air reactor where it is re-oxidized by oxygen from air and circulated back to complete the loop.

Early research in the area of chemical-looping combustion focused primarily on the use of gaseous fuels such as natural gas and syngas. However, the use of coal for CLC has garnered significant interest in recent years. In the real world operation of coal-direct CLC (CD-CLC), the implementation of a spouted fluidized bed fuel reactor offers several technical benefits. The spouted fluidized bed was proposed by Mathur and Gishler (1955) to overcome the limitation of a typical bubbling or fast fluidized bed to handle particles larger than a few hundred micrometers in diameter. Relatively larger particles of the oxygen carrier are beneficial for CD-CLC operation for easier separation of the smaller coal and ash particles from the recirculating oxygen carrier; based on the diameter and density, these particles can be classified as Group D particles according to Geldart's powder classification (1973). The spouted fluidized bed utilizes a high velocity gas stream to create a local high velocity region at the center of the bed (known as the spout) where the particles and voids (bubbles) move in a structured manner with little radial displacement (Sutkar, et al., 2013a).

In the context of CD-CLC, the high velocity jet injection can create strong solid-gas mixing in the spout and high circulation avoiding loss of reactivity due to the ash agglomeration with the oxygen carrier (Rubel, et al., 2011). A significant source of difference in the behavior of a spouted fluidized bed from that of a bubbling or fast fluidized bed are the intense particle-particle and particle-wall collisions. The work of Gryczka et al. (2009) with 2 mm-diameter Geldart Group D-type particles has suggested that accurate numerical representation of particle dynamics is not likely to be achieved for spouted beds using the multiphase granular solid phase approximation due to "the inadequacies of the continuum model." The inaccuracy arises from the non-physical closure terms used in the Eulerian model such as the frictional solids viscosity or the solids pressure based on the kinetic theory of granular flow. To address this, the Lagrangian particle tracking approach known as the Discrete Element Method (DEM) is coupled with CFD simulation of the fluid phase by modeling the interaction between the particles and the fluid individually for each particle. The CFD-DEM coupled simulation can model fluid and particle properties such as position, velocity, temperature, and composition with high accuracy, limited only by the specifics of the particle collision parameters employed in the model.

Recently, simulations using CFD-DEM have proven capable in accurately matching the particle dynamics of various laboratory scale fluidized bed experiments using relatively large particles and in incorporating chemical reactions into the DEM framework(Alobaid, et al., 2013; Banerjee & Agarwal, 2015). The CFD-DEM approach was also employed by Parker (2014) to develop a model of the circulating reactor system at the National Energy Technology Laboratory with reacting flow for CD-CLC. Since the computational cost of the DEM approach is driven by the number of collisions between particles, the cost can be prohibitive when large systems are considered. Industrial scale reactors can contain several trillions of particles; even a laboratory scale experiment can contain particles numbering in the millions. In contrast, the largest number of particles used in a CFD-DEM simulation is 4.5 million in the work of Tsuji et al. (2008), which required months of computing time on 16 CPUs. In order to perform coupled CFD-DEM simulations of CLC reactors in a reasonable time with the laboratory resources available, it is necessary to develop a robust methodology to scale down the number of particles so that the number of collisions is drastically reduced. Fluidized bed scaling based on dynamic similarity provides such a methodology.

A novel dynamic scaling methodology was recently proposed for fluidized beds based on the terminal velocity of the particles (Banerjee & Agarwal, 2016). Simulations of the cold-flow spouted fluidized bed experiment of Sutkar et al. (2013b) using 1-mm-diameter glass particles are used to characterize the performance of the new scaling law in comparison with the scaling methodologies of Glicksman et al. (1993) and Link et al. (2009). It is shown that the new model improves the accuracy of the simulation results compared to the other scaling methodologies while also providing the largest reduction in the number of particles. The dynamic behavior and fluidization in a gas-solid system for CD-CLC depend on the physical properties of the bed material (particle diameter, density, restitution coefficient, etc.). Therefore, it is important to verify the effectiveness of the proposed u_t-based scaling approach for a different bed material. This paper extends the validation of the proposed scaling law for γ-Al_2O_3 particles with significantly different physical properties by comparing the results of the various scaled simulations against the full-scale simulations conducted by Sutkar et al. (2013c) as a follow up to their experimental studies.

2. Description of Experimental Setup

The cold flow experiment of Sutkar et al. (2013b) consists of a pseudo-2D spouted fluidized bed with draft plates as shown in Figure 2. The height *h* is the particle entrainment height below the draft plates; it is set at 0.3 m in the experiments. The draft plates address the problem of spout gas bypassing and spout instability observed in previous work (Banerjee & Agarwal, 2015) by imposing a restriction on the lateral particle flow between the spout and the annulus. By preventing the particles traveling downwards in the annulus from entering the spout and colliding with the particles traveling upwards, the random fluctuations in the spout are eliminated (Claflin & Fane, 1983). In the experiment, a high speed particle image velocimetry (PIV) camera is used to capture the instantaneous particle velocities at various heights. These velocity data are used in this paper to quantitatively compare the performance of the different scaling methodologies.

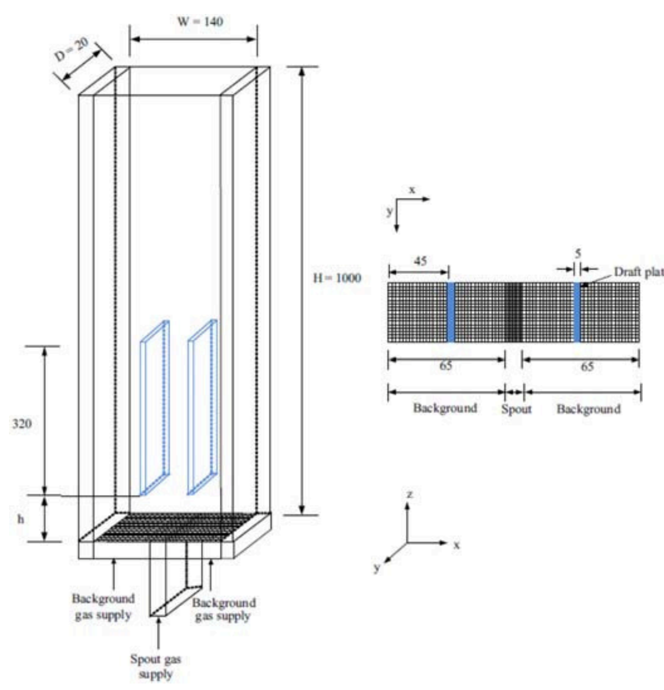

Figure 2. Geometry of the spouted fluidized bed experiment of Sutkar et al. (Sutkar, et al., 2013b)

Sutkar et al. (2013b) employed 1-mm-diameter particles made of glass with a density of 2,500 kg/m³ or γ-Al_2O_3 particles with a density of 1,040 kg/m³ as the bed material in their experiments. The goal of the experiment was to map the flow regime as a function of the ratios of the spout velocity and the background flow velocity to the minimum fluidization velocity of the particles. In this paper, only the "fluidized bed-spouting with aeration" condition is considered since it is the flow regime better suited for CD-CLC operation. Since PIV velocity data is not available for the γ-Al_2O_3 particles, the results of the scaled simulations in this paper are compared againstthe full-scale numerical study conducted as a follow-up to the experiment by the same group (Sutkar, et al., 2013c).

3. Numerical Solution Approach

The simulations in this paper are performed using the commercial CFD solver ANSYS Fluent, release version 14.5 (2012a; 2012b). The flow field is computed using the Navier-Stokes equations of fluid motion; the motion of the particles is obtained using Newton's second law. In order to achieve a coupled CFD-DEM simulation for the multiphase flow, source terms are introduced in the Navier-Stokes momentum equation to capture the solid-gas momentum exchange and in the Newtonian equation of motion to account for forces on the solid particles due to the fluid.

3.1. Equations of Motion for CFD-DEM

The Navier-Stokes equations of fluid motion are slightly modified to account for the presence of the solid particles by including the porosity or fluid volume fraction α_f in the computational cell where the equations are applied. The continuity equation and momentum equations for the cold flow simulation are given by

$$\frac{\partial}{\partial t}(\alpha_f \rho_f) + \nabla \cdot (\alpha_f \rho_f \boldsymbol{u}_f) = 0 \tag{1}$$

$$\frac{\partial}{\partial t}(\alpha_f \rho_f \boldsymbol{u}_f) + \nabla \cdot (\alpha_f \rho_f \boldsymbol{u}_f \boldsymbol{u}_f) = -\alpha_f \nabla p_f - \nabla \cdot \bar{\bar{\tau}}_f + \alpha_f \rho_f \mathbf{g} - \boldsymbol{R}_{sg} \tag{2}$$

For an incompressible Newtonian fluid, the shear stress tensor $\bar{\bar{\tau}}_f$ is simply the Cauchy stress tensor with zero bulk viscosity

$$\bar{\bar{\tau}}_f = \mu_f \left[\left(\nabla \boldsymbol{u}_f + \nabla \boldsymbol{u}_f^T \right) - \frac{2}{3} \nabla \cdot \boldsymbol{u}_f \bar{\bar{I}} \right] \tag{3}$$

The source term R_{sg} in Eq. (2) accounts for the gas-solid momentum exchange and is obtained from the average of the drag forces acting on all the discrete particles in the given computational cell. The energy equation is not applicable for cold flow simulations.

The trajectory of each particle is computed by integrating the force balance on the particle, which can be written in the Lagrangian frame per unit particle mass as

$$\frac{\partial \boldsymbol{u}_p}{\partial t} = \mathbf{g} \frac{(\rho_f - \rho_p)}{\rho_p} + F_D(\boldsymbol{u}_f - \boldsymbol{u}_p) + \boldsymbol{F}_C \tag{4}$$

where the subscript p denotes an individual particle. The terms on the right hand side of Eq. (4) account for the gravitational and buoyant forces, the drag force, and an additional force due to particle-particle or particle-wall collisions. Forces such as the virtual mass force and pressure gradient force can be neglected for gas-solid flows given ρ_p far exceeds ρ_f. The net drag coefficient F_D is given by

$$F_D = \frac{18\mu_f}{\rho_p d_p^2} \frac{C_D Re_p}{24} \tag{5}$$

where d_p is particle diameter, C_D is the particle drag coefficient, and Re_p is the Reynolds number based on the particle diameter defined as

$$\mathrm{Re}_p = \frac{\rho_f d_p |\boldsymbol{u}_f - \boldsymbol{u}_p|}{\mu_f} \tag{6}$$

The drag coefficient can be modeled using various empirical relations. The drag law proposed by Syamlal and O'Brien (Syamlal & O'Brien, 1989) is selected for the spouted fluidized beds simulations in this paper. The Syamlal-O'Brien drag law is a good choice because it uses a correction based on the terminal velocity of the particle, which is the minimum velocity that is large enough to lift the particle out of the bed and is an important parameter for characterizing a spouted bed. The Syamlal O'Brien drag law defines

$$C_D = \left(0.63 + \frac{4.8}{\sqrt{\mathrm{Re}_p / v_{r,p}}} \right)^2 \tag{7}$$

In Eq. (7), $v_{r,p}$ is the terminal velocity correction for the particulate phase given by

$$v_{r,p} = 0.5 \left(A - 0.06\,\mathrm{Re}_p + \sqrt{(0.06\,\mathrm{Re}_p)^2 + 0.12\,\mathrm{Re}_p(2B - A) + A^2} \right) \tag{8}$$

where

$$A = \alpha_f^{4.14} \text{and } B = \begin{cases} 0.8\alpha_f^{1.28} & \text{if } \alpha_f \leq 0.85 \\ \alpha_f^{2.65} & \text{if } \alpha_f > 0.85 \end{cases}$$

In this paper, the collision force in Eq. (4) is computed using the soft-sphere model, which decouples the normal and tangential components. The normal force on a particle involved in a collision is given by

$$\boldsymbol{F}_C^n = (K\delta + \gamma(\boldsymbol{u}_{12}\boldsymbol{e}))\boldsymbol{e} \tag{9}$$

where δ is the overlap between the particle pair involved in the collision as illustrated in Figure 3 and γ is the damping coefficient, a function of the particle coefficient of restitution η; $\boldsymbol{e}$ is the unit vector in the direction of $\boldsymbol{u}_{12}$. Previousresearch by Link has demonstrated that for large values of K, the results of the soft-sphere model are identical to those obtained using a hard-sphere model (Link, 1975). The tangential collision force is a fraction μ of the normal force with μ as a function of the relative tangential velocity v_r given as

$$\mu(v_r) = \begin{cases} \mu_{stick} + (\mu_{stick} - \mu_{glide})(v_r/v_{glide} - 2)(v_r/v_{glide}) & \text{if } v_r < v_{glide} \\ \mu_{glide} & \text{if } v_r \geq v_{glide} \end{cases} \tag{10}$$

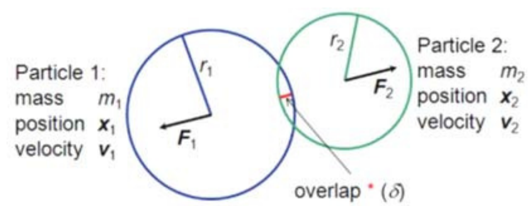

Figure 3. Schematic of particle collision model for DEM(ANSYS, 2012b)

3.2. Scaling Methodologies

For a typical CD-CLC system, the computational cost of tracking each individual particle is prohibitive. One simple approach available in ANSYS Fluent for reducing the computing load is to divide the particles into clusters called parcels. The motion of each parcel is determined as a whole by tracking a single representative particle(ANSYS, 2012b). Parcel collisions are evaluated in the same manner as shown in Figure 3 but the mass of the entire parcel is considered, not just that of a single representative particle. The parcel diameter is that of a sphere whose volume is the sum of the volumes of its constituent particles. Hence, specifying a parcel diameter equal to twice the particle diameter leads to a reduction in the number of objects tracked by the DEM solver by a factor of eight, with an even larger decrease in the number of collisions.

3.2.1 Scaling Methodology of Glicksman et al. (1993)

The parcel approach provides a good starting point in reducing the computational cost of the coupled CFD-DEM simulation. More robust scaling methodologies can be derived based on the principles of dynamic similarity. By non-dimensionalizing the governing equations of multiphase flow, Glicksman(1984) determined thecontrolling non-dimensional parameters for gas-solid flows. One equation of note is the Ergun equation, which predicts the gas-solid momentum exchange coefficient considering both viscous and inertial effects.

$$\frac{\Delta p}{L} = 1.75 \frac{\rho_f (1 - \alpha_f) u_0^2}{d_p \alpha_f^3} + 150 \frac{\mu_f (1 - \alpha_f)^2 u_0}{d_p^2 \alpha_f^3} \tag{11}$$

The full set of scaling parameters were simplified by Glicksman et al. (1993) by isolating the viscous and inertialterms on the right hand side of the Ergun equation. The simplified parameters hold exactly at both low and high values of Re_p (i.e., for both viscosity-dominated and inertia-dominated gas-solid flows) and are reasonably accurate for the entire range of conditions where the Ergun equation is applicable for obtaining the interphase momentum exchange. They are particularly applicable to a spouted fluidized bed because the relatively large particle diameters and high fluidization velocity places such a system in the inertia-dominated regime. Glicksman et al. (1993) proposed a scaling methodology where the dimensions of the fluidized bed are reduced and the superficial velocity u_0 is adjusted accordingly to maintain the same Froude number, Fr = ($u_0/\sqrt{gL}$) Assuming a geometry scale *r* with the subscripts ex and sc representing the exact and scaled systems respectively, the square of the Froude number can be written as

$$\frac{u_{0,ex}^2}{gL_{ex}} = \frac{u_{0,sc}^2}{gL_{sc}} \Rightarrow \frac{u_{0,ex}}{u_{0,sc}} = \left(\frac{L_{ex}}{L_{sc}}\right)^{1/2} = r^{1/2} \quad (12)$$

In turn, the minimum fluidization velocity u_{mf} is adjusted by reducing the particle diameter to hold u_0/u_{mf} constant. By definition, the minimum fluidization velocity occurs when the pressure drop in the Ergun equation is equal to the gravitational force of the particle bed, as given by

$$g(\rho_p - \rho_f) = 1.75\frac{\rho_f u_{mf}^2}{d_p \alpha_f^3} + 150\frac{\mu_f(1-\alpha_f)u_{mf}}{d_p^2 \alpha_f^3} \quad (13)$$

After calculating the minimum fluidization velocity for the original model, the particle scaling factor *n* can be found by substituting for the minimum fluidization velocity in Eq. (13) and rearranging to solve the quadratic equation for *n* given as

$$g(\rho_p - \rho_f)n^2 - \frac{1.75\rho_f(1-\alpha_f)(r^{1/2}u_{mf,ex}^2)}{d_{p,ex}\alpha_f^3}n - \frac{150\mu_f(1-\alpha_f)^2(r^{1/2}u_{mf.ex})}{d_{p,ex}^2\alpha_f^3} = 0 \quad (14)$$

Glicksman et al. (1993) demonstrated the utility of their scaling methodology by considering 1/4 and 1/16 scale models of an experimental reactor and matching the solid fraction profiles across the systems. In the context of CFD-DEM, the simplified scaling methodology of Glicksman et al. (1993) holds promise because the reduction in particle diameter is smaller than the geometry scale used, allowing for a reduction in the total number of particles required in the system to maintain the same bed height. From Eq. (14), given the properties of glass beads and air and a geometry scale of 1/4, the particle diameter must be scaled by 0.62, resulting in a reduction in the number of particles by a factor of around 15 (= $(0.62/0.25)^3$).

3.2.2. Scaling Methodology of Link et al. (2009)

The scaling approach of Glicksman et al. (1993) was derived for scaling experimental fluidized beds to reduce cost; its applicability to CFD-DEM simulations due to the reduction in the number of particles is coincidental.It should be noted that the particle Reynolds number, Re_p and the Archimedes number, Ar (the ratio of gravitational forces to inertial forces) for the scaled system according to Glicksman et al. (1993) are roughly equal to 0.34 and 0.12 times their exact values for the 1/4 and 1/16 scaled models respectively in the limit of very small particles; for the larger particles, the difference is even greater and varies with particle density. The ratio of the superficial velocity to the terminal velocity of the particles u_0/u_t is also significantly decreased. These are important parameters for accurately capturing the fluidization behavior for a spouted bed that cannot be matched by the Glicksman scaling law.

Link et al. (2009) proposed a scaling methodology for CFD-DEM simulation that utilizes the ability to change the physical properties of the materials in a computational model, which is not possible in an experiment, in order to maintain the same Re_p and Ar in the scaled model. By keeping these two parameters the same, the u_{mf} is also held constant. Unlike Glicksman, the scaling approach proposed by Link et al. (2009) only scales up the particle diameter while retaining the original geometry. Hence, Fr remains constant without changing u_0 and the other scaling parameter used by Glicksman et al. (1993),u_0/u_{mf}, is automatically matched. By increasing the particle diameter by a factor of n, the number of particles can be reduced by a factor of n^3 while maintaining the same particle volume. To maintain the same particle Reynolds number, the dynamic viscosity for the gas phase in the scaled simulation is defined as

$$Re_{p,sc} = Re_{p,ex} \Rightarrow \mu_{f,sc} = \frac{d_{p,sc}}{d_{p,ex}}\mu_{f,ex} = n\mu_{f,ex} \quad (15)$$

given that the fluid density does not change. In the same vein, the Archimedes number can be held constant by setting a new particle density for the scaled simulation

$$Ar = \frac{gd_p^3}{\mu_f^2}(\rho_p - \rho_f);\ Ar_{sc} = Ar_{ex} \Rightarrow \rho_{p,2} = \frac{(\rho_{p,1} - \rho_{f,1})}{n} + \rho_{f,2} \quad (16)$$

3.2.3 Novel Scaling Methodology based on Terminal Velocity

The scaling law of Link et al. (2009) addresses the shortcoming of the simplified Glicksman scaling law (1993) by maintaining the same Re_p and Ar between the original and scaled models as well as by maintaining the same Fr and u_0/u_{mf}. Unfortunately, the ratio u_0/u_t, a crucial parameter in defining the fluidization behavior in a fluidized bed is reduced to 0.707 of its original value, which can be expected to reduce the spout velocity of the particles in the scaled system. To rectify this, a new scaling methodology is proposed in this paper to keep u_0/u_t constant in addition to every other non-dimensional parameter used in the other two scaling methodologies.

Hence, the final set of scaling parameters used in the novel approach are Fr and u_0/u_{mf} from the simplified scaling law of Glicksman et al. (1993), Re_p and Ar from the scaling law of Link et al. (2009) and u_0/u_t. First, thegeometry is scaled by a factor r and u_0 by a factor of $r^{(1/2)}$ as in Eq. (12) to keep Fr constant. Similar to Link et al. (2009), the physical properties of the materials are changed to match certain non-dimensional parameters independently while not affecting others. In this case, the fluid density is changed depending on the particle scaling factor *n* (yet to be determined) to keep Re_p constant given the change in u_0, therefore

$$Re_{p,sc} = Re_{p,ex} \Rightarrow \rho_{f,sc} = \rho_{f,ex}\frac{d_{p,ex}}{d_{p,sc}}\frac{u_{0,ex}}{u_{0,sc}} = \frac{\rho_{f,ex}}{nr^{1/2}} \quad (17)$$

For typical values of Re_p for a spouted fluidized bed, the terminal velocity is defined as

$$u_t^2 = 3\frac{(\rho_p - \rho_f)gd_p}{\rho_f} \quad (18)$$

After calculating the terminal velocity for the original model, one can determinenby substituting for the scaled fluid density and terminal velocity in Eq. (18) and rearranging to solve the quadratic equation for n given as

$$\rho_p n^2 - \frac{\rho_{f,ex}}{r^{1/2}}n - \frac{1}{3}\frac{\rho_{f,ex}u_{t,ex}^2 r^{1/2}}{gd_{p,ex}} = 0 \quad (19)$$

Using the particle scaling factor determined by Eq. (19) and the corresponding scaling for the fluid's density given by Eq. (17), Ar for the scaled model can be found to be equal to its original value and the ratio u_0/u_{mf} is automatically matched. Of the three scaling methodologies as well as the parcel approach discussed in this section, it is expected that this novel approach will most closely reproduce the fluidization behavior of the original scale experiment in the scaled simulation because it retains the same values for a larger set of non-dimensional parameters.

4. Computational Setup

Four different cases are considered that reduce the total number of particles in the bed: the parcel approach, the Glicksman scaling law (1993), the Link scaling law (2009), and the proposed scaling law based on the terminal velocity. As discussed in section 3.2, the independent variable for the parcel approach and the Link scaling law is the particle scale factor *n*. A value of *n* = 2 is chosen for the current simulations while keeping the bed geometry the same. On the other hand, the independent variable for the Glicksman scaling law and the proposed scaling law is the geometry scale factor r; it is set at *r* = 0.25 in line with Glicksman et al. (1993) and the particle scale is adjusted as determined by the respective scaling methodology. In all four cases, u_{sp} and u_{bg} are set at roughly 37.0u_{mf} and 1.275u_{mf} respectively in accordance with the experiment to model the "fluidized bed-spouting with aeration" flow regime. Although the flow in the spouted fluidized bed setup is turbulent, it is well-established that for gas-solid flows, the effect of turbulence is increasingly negligible compared to the effect of the solids for solid volume fractions above 0.001 (Elgobashi, 1994). For the simulations in this paper, the effect of turbulence can be ignored without loss of accuracy in line with the previous work using the CFD-DEM approach (Parker, 2014). The initial bed height (equal to the bed width) is achieved by releasing a large number of particles into the bed prior to the start of each simulation. The different simulation cases considered in this paper and the simulation parameters are summarized in Table 1.

The particle scaling factor n for the parcel approach in Table 1 is the ratio between the parcel diameter and the particle diameter. The parcel approach reduces the computing cost by considering a single representative

Table 1. Summary of scaled test cases with γ-Al_2O_3 particles with adjusted physical properties of gases and solids and comparison of non-dimensional parameters with the exact scale

Case		B1	B2	B3	B4
Parameter	Exact scale	Parcel approach	Glicksman scaling law	Link scaling law	Proposed u_t-based scaling law
n	1	$2^{\dagger}$	0.62	2	0.708
r	1	1	0.25	1	0.25
ρ_p, kg/m³	1040	1040	1040	520.6	1040
ρ_f, kg/m³	1.225	1.225	1.225	1.225	3.461
μ_f, kg/(m-s)	1.79E-05	1.79E-05	1.79E-05	3.58E-05	1.79E-05
u_{mf}, m/s	0.36	0.36	0.18	0.36	0.18
u_t, m/s	4.99	4.99	2.88	4.99	2.49
u_{bg}, m/s	0.46	0.46	0.23	0.46	0.23
u_{sp}, m/s	13.2	13.2	0.66	13.2	6.6
$\frac{(u_0/u_{mf})_{sc}}{(u_0/u_{mf})_{ex}}$	1	N/A	1	1	1
$\frac{Re_{p,sc}}{Re_{p,ex}}$	1	N/A	0.310	1	1
$\frac{Ar_{sc}}{Ar_{ex}}$	1	N/A	0.239	1	1
$\frac{(u_0/u_t)_{sc}}{(u_0/u_t)_{ex}}$	1	N/A	0.711	0.707	1
Total # particles	460k	51k	23k	51k	17k
Particle time step, s	–	2e-5	5e-6	2e-5	5e-6

particle within each parcel to calculate the motion of the parcel. As such, a direct comparison between the non-dimensional numbers does not apply for the parcel approach. It should be noted that for the 1/4 scale models, because of the reduced particle size, the particle time step is reduced from 2e 5 seconds to 5e 6 seconds to ensure that the particle collisions are accurately resolved. This increase in computational cost is more than offset by the reduced number of particles to track, and is further offset by the coarser mesh required for the 1/4 scaled models to ensure that the particle volume remains smaller than the minimum cell volume. Given that the goal of the scaling methodology is to reduce the computing cost of the CFD-DEM simulation, the reduction in the total number of particles from roughly 461,000 in the original scale system is an important parameter for evaluating the performance of the scaling methodology. The reduction in the number of particles is the cube of the ratio of the particle scale factor n to the geometry scale factor r. For each case, a greater reduction can be achieved by increasing the independent scaling factor, but a drastic increase can alter the fluidization behavior of the system (e.g., the particles may no longer fall in the spoutable range). For the simulation cases considered, the proposed u_t-based scaling law requires the fluid density ρ_f to be increased from 1.225 kg/m³ to 3.461 kg/m³ to ensure the non-dimensional parameters in the scaled model match the actual case. This increase in ρ_f is only slightly greater than the scaling adjustment made to the particle density ρ_p in the scaling law of Link et al. (2009) even though the existing law required a further scaling of the fluid viscosity μ_f by the same factor. It can be seen from Table 1that the proposed μ_t-based scaling law also offers the largest reduction in the number of particles by up to 95% leading to substantial reductions in the computing time in both cases.

The computational domain used in the simulations is an exact representation of the experimental apparatus of Sutkar et al. (2013b) shown in Figure 3. A quarter-scale domain is used for simulations using the Glicksman and the proposed novel scaling approaches (r = 0.25). A structured mesh is generated with 24,000 cells for the original scale model and 4,000 cells for the 1/4 scale model. The difference in number is to ensure that the minimum cell volume remains greater than the particle volume for each simulation, a constraint imposed by the CFD-DEM approach. The meshes used in the simulations conducted in this paper are shown in Figure 4. Particle velocity data in the z-direction is recorded in the central xz-plane at heights of 30 cm and 50 cm (7.5 cm and 12.5 cm in the 1/4 scale models) for comparison with the full-scale simulations conducted by Sutkar et al. (2013c).

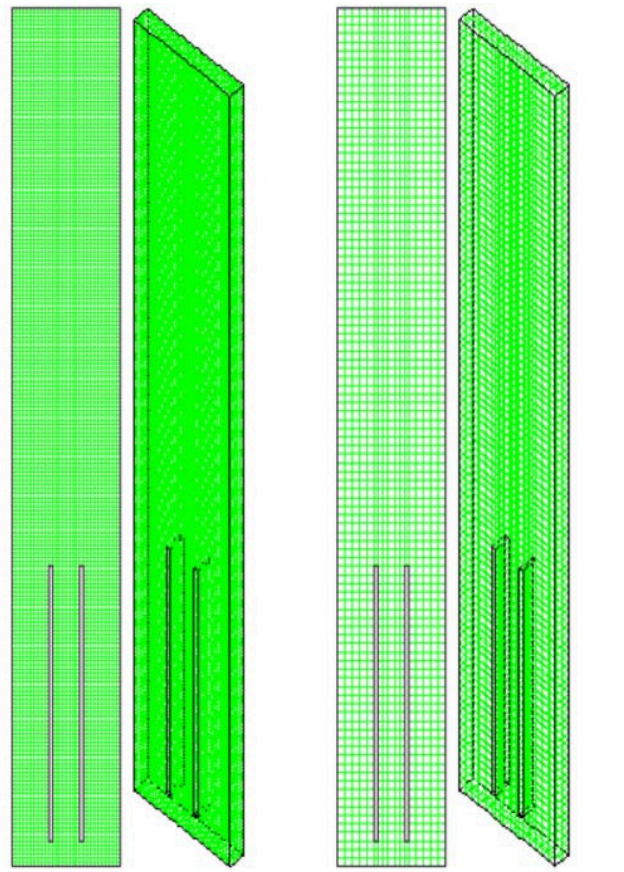

Figure 4. Computational mesh for original scale model (left) and the 1/4 scale model (right)

5. Results and Discussion

For simulates with the glass beads conducted in previous work (Banerjee & Agarwal, 2016), the proposed u_t-based scaling law outperforms the other scaling approaches and provides the best match with the experimental values. However, since the dynamic behavior and fluidization in a gas-solid system for CLC depend on the physical properties of the bed material (particle diameter, density, restitution coefficient, etc.), it is important to verify the effectiveness of the proposed u_t-based scaling approach for a different bed material. The γ-Al_2O_3 particles considered in this paper have the same diameter as the glass beads but lower density and restitution coefficient of 1040 kg/m³ and 0.74 respectively compared to 2500 kg/m³ and 0.97 for glass. The time-averaged particle velocity of the γ-Al_2O_3 particles in the z-direction for simulation cases B1-B4 is recorded at heights of 10 cm and 30 cm respectively and compared against the results from the full-scale simulation of Sutkar et al. (2013c). The velocity profiles using the different scaling methodologies listed in Table 1 at 10 cm and 30 cm are presented in Figure 5 and Figure 6 respectively.

It is noted that the full-scale simulations results shown in Figure 5 and Figure 6 are asymmetric due to the way the boundary conditions were imposed (Sutkar, et al., 2013c); similar asymmetry could be observed in the particle tracks and velocity profiles for glass beads as well. As such, only the magnitude of the velocities in the full-scale simulation results should be considered for comparing the scaling methodologies, not the profile shape. At z=10 cm, there is a strong spout in the central region but the particles in the annulus are densely packed. On the other hand, at z=30 cm, the spout velocities are weaker but there is a distinct downwards motion of the particles in the annulus. In both Figure 5 and Figure 6, the Link scaling law and the proposed u_t-based scaling provide the best match with the full-scale simulation results; the parcel approach and the Glicksman scaling law under-predict the spout velocity. All the scaling laws capture the densely packed bed with no particle velocity in the annulus as shown

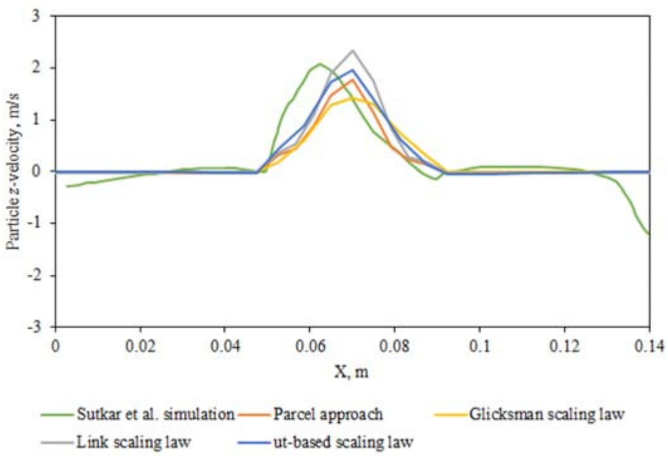

Figure 5. Time-averaged particle z - velocity at z = 10 cm for scaled simulation cases B1–B4 compared with full-scale simulation results (Sutkar, et al., 2013c)

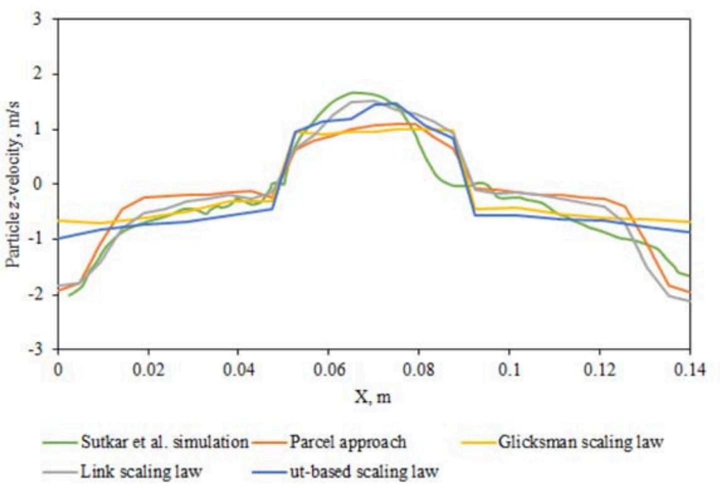

Figure 6. Time-averaged particle z-velocity at z =30 cm for scaled simulation cases B1–B4 compared with full-scale simulation results (Sutkar, et al., 2013c)

in Figure 5. However, the proposed u_t-based scaling law better captures the gradual change in particle z-velocities in the annular region in Figure 6; the Link scaling law shows a nearly zero velocity in much of the annulus before producing a sharp decrease towards the edges. Once again, the proposed scaling law can be seen to produce the best match with the full-scale simulation results on top of providing the largest reduction in the number of particles.

6. Conclusion

The parcel approach, the simplified scaling law of Glicksman et al. (1993), the scaling law of Link et al. (2009), and the proposed u_t-based scaling law have been used to simulate an experimental spouted fluidized bed with draft plates using the CFD-DEM approach. The particle velocity is an important quantity for characterizing the fluidization behavior in a spouted fluidized bed; it is used in this paper to compare the performance of the different scaling approaches. Comparing the particle velocities in the z-direction at various heights, it is found that all the scaling methodologies can capture the general trends in the particle velocities at different heights to varying degrees of accuracy. As with the previous simulations with glass beads, the proposed u_t-based scaling law outperforms the other scaling approaches and provides the best match with the experimental values for the γ-Al_2O_3 particles considered in this paper. As such, the proposed scaling law is affirmed to be the ideal scaling methodology for a spouted fluidized bed for a wide range of bed materials. This makes sense because the scaled model using the proposed approach maintains the same values as the experiment for all the non-dimensional parameters used to ensure dynamic similarity. The proposed scaling law also provides the largest reduction in the number of particlesin the system in all cases, and in turn, the largest reduction in computing cost. The establishment of a scaling law that can maintain fidelity with experiment is a crucial step towards the development of CFD-DEM simulations of industrial scale fluidized beds for chemical looping combustion.

7. References

Alobaid, F., Ströhle, J. & Epple, B., 2013. Extended CFD/DEM model for the simulation of circulating fluidized bed. Adv. Powder Technol., 24(1), pp. 403-415.

ANSYS, 2012a. ANSYS Fluent User's Guide, Canonsburg, PA: ANSYS, Inc..

ANSYS, 2012b. ANSYS Fluent Theory Guide, Canonsburg, PA: ANSYS, Inc..

Banerjee, S. & Agarwal, R. K., 2015. Transient reacting flow simulation of spouted fluidized bed for coal-direct chemical looping combustion. J. Thermal Sci. Eng. Appl., 7(2), p. 021016.

Banerjee, S. & Agarwal, R. K., 2016. Characterization of scaling laws in computational fluid dynamics simulations of spouted fluidized beds for chemical looping combustion. Energy Fuels.

Claflin, J. K. & Fane, A. G., 1983. Spouting with a porous draft-tube. Canadian J. Chem. Eng., Volume 61, p. 356-363.

Elgobashi, S. E., 1994. On predicting particle-laden turbulent flows. Applied Scientific Research, Volume 52, p. 309-329.

Geldart, D., 1973. Types of gas fluidization. Powder Technol., 7(5), pp. 285-292.

Glicksman, L. R., 1984. Scaling relationships for fluidized beds. Chem. Eng. Sci., 39(9), p. 1373-1379.

Glicksman, L. R., Hyre, M. & Woloshun, K., 1993. Simplified scaling relationships for fluidized beds. Powder Technol., Volume 77, p. 177-199.

Gryczka, O. et al., 2009. Characterization and CFD modeling of the hydrodynamics of a prismatic spouted bed apparatus. Chem. Eng. Sci., Volume 64, p. 3352-3375.

IPCC, 2007. Climate Change 2007: Synthesis Report. Contribution of Working Groups I, II and III to the Fourth Assessment Report of the Intergovernmental Panel on Climate Change [Core Writing Team, Pachauri, R.K., and Reisinger, A. (eds.)], Geneva, Switzerland: IPCC.

Link, J. M., 1975. Development and validation of a discrete particle model of a spout-fluid bed granulator, Enschede, The Netherlands: Ph.D. dissertation, University of Twente.

Link, J. M. et al., 2009. Comparison of fibre optical measurements and discrete element simulations for the study of granulation in a spout fluidized bed. Powder Technol., Volume 189, p. 202-217.

Mathur, K. B. & Gishler, P. E., 1955. A technique for contacting gases with coarse solid particles. AIChE J., Volume 157-164, p. 1.

Parker, J., 2014. CFD model for the simulation of chemical looping combustion. Powder Technol., Volume 265, p. 47-53.

Rubel, A., Zhang, Y., Liu, K. & Neathery, J., 2011. Effect of ash on oxygen carriers for the application of chemical looping combustion to a high carbon char. Oil Gas Sci. Technol. - Rev. IFP Energies Nouv., 66(2), pp. 291-300.

Sutkar, V. S., Deen, N. G. & Kuipers, J. A. M., 2013a. Spout fluidized beds: Recent advances in experimental and numerical studies. Chem. Eng. Sci., Volume 86, p. 124-136.

Sutkar, V. S. et al., 2013c. Numerical investigations of a pseudo-2D spout fluidized bed with draft plates using a scaled discrete particle model. Chem. Eng. Sci., Volume 104, p. 790-807.

Sutkar, V. S. et al., 2013b. Experimental investigations of a pseudo-2D spout fluidized bed with draft plates. Chem. Eng. Sci., Volume 102, p. 524-543.

Syamlal, M. & O'Brien, T. J., 1989. Computer simulation of bubbles in a fluidized bed. AIChE Symp. Ser., Volume 85, p. 22-31.

Tsuji, T., Yabumoto, K. & Tanaka, T., 2008. Spontaneous structures in three-dimensional bubbling gas-fluidized bed by parallel DEM-CFD coupling simulation. Powder Technol., 184(2), p. 132-140.